3 The atmospheric boundary layer and wind turbulence

3.1 Introduction

As the earth's surface is approached, the frictional forces play an important role in the balance of forces on the moving air. For larger storms such as extra-tropical depressions, this zone extends up to 500 to 1000 m height. For thunderstorms, the boundary layer is much smaller – probably around 100 m (see Section 3.2.5). The region of frictional influence is called the 'atmospheric boundary layer' and is similar in many respects to the turbulent boundary layer on a flat plate or airfoil at high wind speeds.

Figure 3.1 shows records of wind speeds recorded at three heights on a tall mast at Sale in southern Australia (as measured by sensitive cup anemometers, during a period of strong wind produced by gales from a synoptic depression (Deacon, 1955). The records show the main characteristics of fully-developed 'boundary-layer' flow in the atmosphere:

- the increase of the average wind speed as the height increases
- the gusty or turbulent nature of the wind speed at all heights
- the broad range of frequencies in the gusts in the air flow
- there is some similarity in the patterns of gusts at all heights, especially for the more slowly changing gusts, or lower frequencies.

The term 'boundary-layer' means the region of wind flow affected by friction at the earth's surface, which can extend up to 1 km. The Coriolis forces (Section 1.2.2) become gradually less in magnitude as the wind speed falls near the earth's surface. This causes the geostrophic balance, as discussed in Chapter 1 to be disturbed, and the mean wind vector turns from being parallel to the isobars to having a component towards low pressure,

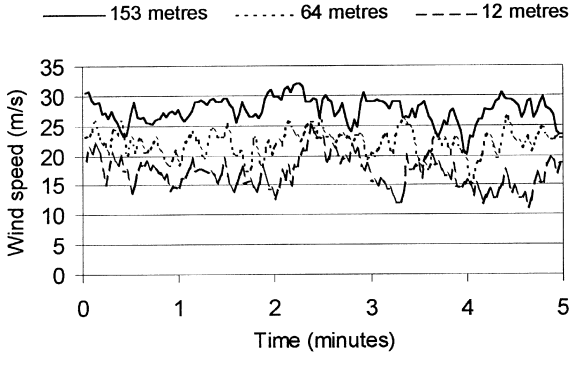

Figure 3.1 Wind speeds at three heights during a gale (Deacon, 1955).

as the height above the ground reduces. Thus the mean wind speed may change in direction slightly with height, as well as magnitude. This effect is known as the *Ekman Spiral*. However the direction change is small over the height range of normal structures, and is normally neglected in wind engineering.

The following sections will mainly be concerned with the characteristics of the mean wind and turbulence, near the ground, produced by severe gales in the higher latitudes. These winds have been studied in detail for more than forty years and are generally well understood, at least over flat homogeneous terrain. The wind and turbulence characteristics in tropical cyclones (Section 1.3.2) and thunderstorm downbursts (Section 1.3.5), which produce the extreme winds in the lower latitudes, are equally important, but are much less well understood. However, existing knowledge of their characteristics is presented in Sections (3.2.5) and (3.2.6).

3.2 Mean wind speed profiles

3.2.1 The 'logarithmic law'

In this section we will consider the variation of the mean or time-averaged wind speed with height above the ground near the surface (say in the first 100–200 m – the height range of most structures). In strong wind conditions, the most accurate mathematical expression is the 'logarithmic law'. The logarithmic law was originally derived for the turbulent boundary layer on a flat plate by Prandtl; however it has been found to be valid in an unmodified form in strong wind conditions in the atmospheric boundary layer near the surface. It can be derived in a number of different ways. The following derivation is the simplest, and is a form of dimensional analysis.

We postulate that the wind shear, i.e. the rate of change of mean wind speed, $\bar{U}$, with height is a function of the following variables:

- the height above the ground, z
- the retarding force per unit area exerted by the ground surface on the flow – known as the surface shear stress, τ_0
- the density of air, ρ_a

Note that near the ground, the effect of the earth's rotation (Coriolis forces) is neglected. Also because of the turbulent flow, the effect of molecular viscosity can be neglected.

Combining the wind shear with the above quantities, we can form a non-dimensional wind shear:

$$\frac{d\bar{U}}{dz} z \sqrt{\frac{\rho_a}{\tau_0}}$$

$\sqrt{(\tau_0/\rho_a)}$ has the dimensions of velocity, and is known as the *friction velocity*, u_* (note that this is not a physical velocity). Then, since there are no other non-dimensional quantities involved,

$$\frac{dU}{dz} \frac{z}{u_*} = \text{a constant, say } \frac{1}{k} \tag{3.1}$$

Integrating,

$$\bar{U}(z) = \frac{u_*}{k}(\log_e z - \log_e z_0) = \frac{u_*}{k}\log_e(z/z_0) \tag{3.2}$$

where z_0 is a constant of integration, with the dimensions of length, known as the *roughness length*.

Equation (3.2) is the usual form of the logarithmic law. k is known as *von Karman's constant*, and has been found experimentally to have a value of about 0.4. z_0, the roughness length, is a measure of the roughness of the ground surface.

Another measure of the terrain roughness is the *surface drag coefficient*, κ, which is a non-dimensional surface shear stress, defined as:

$$\kappa = \frac{\tau_0}{\rho \bar{U}_{10}^2} = \frac{u_*^2}{\bar{U}_{10}^2} \tag{3.3}$$

where $\bar{U}_{10}$ is the mean wind speed at 10 m height.

For urban areas and forests, where the terrain is very rough, the height, z, in equation (3.2) is often replaced by an effective height, $(z - z_h)$, where z_h is a 'zero-plane displacement'. Thus in this case,

$$\bar{U}(z) = \frac{u_*}{k}\log_e\left[\frac{z - z_h}{z_0}\right] \tag{3.4}$$

The zero-plane displacement can be taken as about three-quarters of the general rooftop height.

Usually the most useful way of applying equation (3.4) is to use it to relate the mean wind speeds at two different heights, as follows:

$$\frac{\bar{U}(z_1)}{\bar{U}(z_2)} = \frac{\log_e[(z_1 - z_h)/z_o]}{\log_e(z_2 - z_h)/z_o]} \tag{3.5}$$

In the application of equation (3.3), the 10 m reference height should be taken as ten metres above the zero-plane displacement, or $(10 + z_h)$ metres above the actual ground level.

By applying equations (3.3) and (3.4) for z equal to 10 m, a relationship between the surface drag coefficient and the roughness length can be determined:

$$\kappa = \left[\frac{k}{\log_e\left(\frac{10}{z_o}\right)}\right]^2 \tag{3.6}$$

Table 3.1 gives the appropriate value of roughness length and surface drag coefficient, for various types of terrain types (adapted from the Australian Standard for Wind Loads, AS1170.2, 1989).

Although the logarithmic law has a sound theoretical basis, at least for fully developed wind flow over homogeneous terrain, these ideal conditions are rarely met in practice.

Table 3.1 Terrain types, roughness length and surface drag coefficient

Terrain type	*Roughness length (m)*	*Surface drag coefficient*
Very flat terrain (snow, desert)	0.001–0.005	0.002–0.003
Open terrain (grassland, few trees)	0.01–0.05	0.003–0.006
Suburban terrain (buildings 3–5 m)	0.1–0.5	0.0075–0.02
Dense urban (buildings 10–30 m)	1–5	0.03–0.3

Also the logarithmic law has some mathematical characteristics which may cause problems: first, since the logarithms of negative numbers do not exist, it cannot be evaluated for heights, z, below the zero-plane displacement z_h, and if $z - z_h$ is less than z_o, a negative wind speed is given. Secondly, it is less easy to integrate. To avoid some of these problems, wind engineers have often preferred to use the power law.

3.2.2 The 'power law'

The power law has no theoretical basis but is easily integrated over height – a convenient property when wishing to determine bending moments at the base of a tall structure, for example.

To relate the mean wind speed at any height, z, with that at 10 m (adjusted if necessary for rougher terrains, as described in the previous section), the power law can be written:

$$\bar{U}(z) = \bar{U}_{10}\left(\frac{z}{10}\right)^{\alpha} \tag{3.7}$$

The exponent, α, in equation (3.7) will change with the terrain roughness, and also with the height range, when matched to the logarithmic law. A relationship that can be used to relate the exponent to the roughness length, z_0, is as follows:

$$\alpha = \left(\frac{1}{\log_e(z_{ref}/z_0)}\right) \tag{3.8}$$

where z_{ref} is a reference height at which the two 'laws' are matched. z_{ref} may be taken as the average height in the range over which matching is required, or half the maximum height over which the matching is required.

Figure 3.2 shows a matching of the two laws for a height range of 100 m, using equation (3.8), with z_{ref} taken as 50 m. It is clear the two relationships are extremely close, and that the power law is quite adequate for engineering purposes.

3.2.3 Mean wind profiles over the ocean

Over land the surface drag coefficient, κ, is found to be nearly independent of mean wind speed. This is not the case over the ocean, where higher winds create higher waves, and hence higher surface drag coefficients. The relationship between κ and $\bar{U}_{10}$ has been the subject of much study, and a large number of empirical relationships have been derived.

Charnock (1955), using dimensional arguments, proposed a mean wind profile over the ocean, that implies that the roughness length, z_0, should be given by equation (3.9).

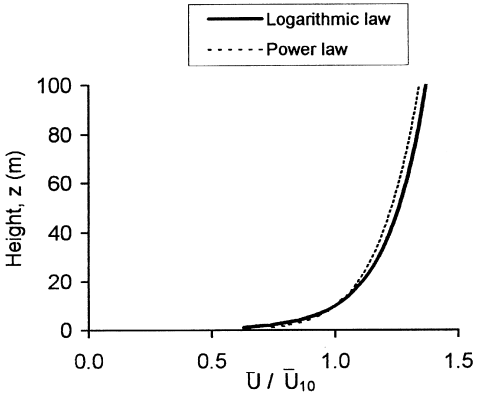

Figure 3.2 Comparison of the logarithmic (z_0 = 0.02 m) and power law (α = 0.128) for mean velocity profile.

$$z_o = \frac{au_*^2}{g} = \frac{a\kappa \bar{U}_{10}^2}{g} \tag{3.9}$$

where g is the gravitational constant, and a is an empirical constant.

Equation (3.9), with the constant a lying between 0.01 and 0.02, is valid over a wide range of wind speeds. It is not valid at very low wind speeds, under aerodynamically smooth conditions, and also may not be valid at very high wind speeds, during which the air-sea surface experiences intensive wave breaking and spray.

Substituting for the surface drag coefficient, κ, from equation (3.6) into equation (3.9), equation (3.10) is obtained.

$$z_o = \frac{a}{g}\left[\frac{k\bar{U}_{10}}{\log_e(10/z_o)}\right]^2 \tag{3.10}$$

z_h is usually taken as zero over the ocean.

The implicit nature of the relationship between z_0 (or κ) and $\bar{U}_{10}$, in equations (3.9) and (3.10) makes them difficult to apply, and several simpler forms have been suggested.

Garratt (1977) examined a large amount of experimental data and suggested a value for a of 0.0144. Using this value for a, taking g equal to 9.81 m/s^2, and k equal to 0.41, the relationship between z_0 and $\bar{U}_{10}$ given in Table 3.2 is obtained.

Table 3.2 Roughness length over the ocean as a function of mean wind speed

$\bar{U}_{10}$ (m/s)	*Roughness length (mm)*
10	0.21
15	0.59
20	1.22
25	2.17
30	3.51

The values given in Table 3.2 can be used in non tropical-cyclone conditions. Mean wind profiles over the ocean in tropical cyclones (typhoons and hurricanes) are discussed in a following section.

3.2.4 Relationship between upper level and surface winds

For large scale atmospheric boundary layers in synoptic winds, dimensional analysis gives a functional relationship between a *geostrophic drag coefficient*, $C_g = u_*/U_g$, and the *Rossby Number*, $Ro = U_g/fz_o$. u_* is the friction velocity and U_g is the geostrophic (Section 1.2.3), or gradient wind; f is the Coriolis parameter (Section 1.2.2) and z_o is the roughness length (Section 3.2.1). Lettau (1959) proposed the following relationship based on a number of full-scale measurements:

$$C_g = 0.16\, Ro^{-0.09} \tag{3.11}$$

Applying the above relationship for a latitude of 40 degrees ($f = 0.935 \times 10^{-4}$) (1/sec.), a value of U_g equal to 40 m/s, and a roughness length of 20 mm, gives a friction velocity of 1.40 m/s and from equation (3.2), a value of $\bar{U}_{10}$ of 21.8 m/s. Thus, in this case, the wind speed near the surface is equal to 0.54 times the geostrophic wind – the upper level wind away from the frictional effects of the earth's surface.

3.2.5 Mean wind profiles in tropical cyclones

A number of low-level flights into Atlantic Ocean and Gulf of Mexico hurricanes were made by the National Oceanic and Atmospheric Administration (N.O.A.A.) of the United States, during the 1970s and 1980s. However the flight levels were not low enough to provide useful data on wind speed profiles below about 200 m. Measurements from fixed towers are also extremely limited. However some measurements were made from a 390 m communications mast close to the coast near Exmouth, Western Australia, in the late 1970s (Wilson, 1979). More recently SODAR (sonic radar) profiles have been obtained from typhoons on Okinawa, Japan (Amano *et al.,* 1999). These show similar characteristics near the regions of maximum winds: a steep logarithmic-type profile up to a certain height (60 to 200 m), followed by a layer of strong convection, with nearly constant mean wind speed.

For design purposes, the following mean wind speed profile may be assumed:

$$\begin{aligned} \bar{U}_{(z)} &= \bar{U}_{10}\frac{\log_e(z/0.3)}{\log_e(10/0.3)} \text{ for } z < 100 \text{ m} \\ \bar{U}_{(z)} &= \bar{U}_{100} \text{ for } z \geq 100 \text{ m} \end{aligned} \tag{3.12}$$

Equation (3.12) is applicable over the ocean, or the adjacent coastline. As the tropical cyclone crosses the coast it weakens (see Chapter 1), and the mean wind profiles would be expected to adjust to the underlying ground roughness. However measurements are virtually non-existent at the present time.

3.2.6 Wind profiles in thunderstorm winds

The most common type of severe wind generated by a thunderstorm is a downburst, discussed in Section 1.3.5. Downbursts may produce severe winds for short periods, and

are transient in nature, and it is therefore meaningless to try to define a 'mean' wind speed for this type of event (see Figure 1.9). However we can separate the slowly varying part, representing the downward airflow which becomes a horizontal 'outflow' near the ground, from any superimposed turbulence of higher frequency.

Thanks to Doppler radar measurements in the U.S.A., and some tower anemometer measurements in Australia and the U.S.A., there are some indications of the wind structure in the downburst type of thunderstorm wind, including the 'macroburst' and 'microburst' types identified by Fujita (1985). At the horizontal location where the maximum gust occurs, the wind speed increases from ground level up to a maximum value at a height of 50–100 m. Above this height, the wind speed reduces relatively slowly.

A useful model of the velocity profiles in the vertical and horizontal directions in a downburst were provided by Oseguera and Bowles (1988). This model satisfies the requirements of fluid mass continuity, but does not include any effect of storm movement. The horizontal velocity component is expressed as equation (3.13).

$$U = \left(\frac{\lambda R^2}{2r}\right)[1 - e^{-(r/R)^2}](e^{-z/z^*} - e^{-z/\varepsilon}) \tag{3.13}$$

where r is the radial coordinate from the centre of the downburst, R is the characteristic radius of the downburst 'shaft', z is the height above the ground, z^* is a characteristic height out of the boundary layer, ε is a characteristic height in the boundary layer and λ is a scaling factor, with dimensions of $[\text{time}]^{-1}$.

The velocity profile at the radius of maximum winds ($r = 1.121R$) is shown in Figure 3.3. The profile clearly shows a maximum at the height of the boundary layer on the ground surface. Radar observations have shown that this height is 50–100 m in actual downbursts.

3.3 Turbulence

The general level of turbulence or 'gustiness' in the wind speed, such as that shown in Figure 3.1, can be measured by its standard deviation, or root-mean-square. First we subtract out the steady or mean component (or the slowly varying component in the case of a transient storm, like a thunderstorm), then quantify the resulting deviations. Since both positive and negative deviations can occur, we first square the deviations before averaging

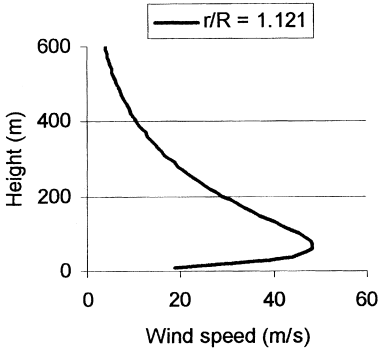

Figure 3.3 Profile of horizontal velocity near the ground during a stationary downburst.

them, and finally the square root is taken to give a quantity with the units of wind speed. Mathematically, the formula for standard deviation can be written:

$$\sigma_u = \left\{ \frac{1}{T} \int_0^T [U(t) - \bar{U}]^2 dt \right\}^{\frac{1}{2}} \tag{3.14}$$

where $U(t)$ is the total velocity component in the direction of the mean wind, equal to $\bar{U} + u(t)$, where $u(t)$ is the 'longitudinal' turbulence component, i.e. the component of the fluctuating velocity in the mean wind direction.

Other components of turbulence in the lateral horizontal direction denoted by $v(t)$, and in the vertical direction denoted by $w(t)$, are quantified by their standard deviations, σ_v, and σ_w, respectively.

3.3.1 Turbulence intensities

The ratio of the standard deviation of each fluctuating component to the mean value is known as the *turbulence intensity* of that component.

Thus,

$$I_u = \sigma_u / \bar{U} \text{ (longitudinal)} \tag{3.15}$$

$$I_v = \sigma_v / \bar{U} \text{ (lateral)} \tag{3.16}$$

$$I_w = \sigma_w / \bar{U} \text{ (vertical)} \tag{3.17}$$

Near the ground in gales produced by large scale depression systems, measurements have found that the standard deviation of longitudinal wind speed, σ_u, is equal to 2.5 u_* to a good approximation, where u_* is the friction velocity (Section 3.2.1). Then the turbulence intensity, I_u, is given by equation (3.18).

$$I_u = \frac{2.5u_*}{(u_*/0.4)\log_e(z/z_0)} = \frac{1}{\log_e(z/z_0)} \tag{3.18}$$

Thus the turbulence intensity is simply related to the surface roughness, as measured by the roughness length, z_o. For a rural terrain, with a roughness length of 0.04 m, the longitudinal turbulence intensity for various heights above the ground are given in Table 3.3, thus the turbulence intensity decreases with height above the ground.

Table 3.3 Longitudinal turbulence intensities for rural terrain (z_o = 0.04 m)

Height, z (m)	I_u
2	0.26
5	0.21
10	0.18
20	0.16
50	0.14
100	0.13

The lateral and vertical turbulence components are generally lower in magnitude than the corresponding longitudinal value. However, for well-developed boundary layer winds, simple relationships between standard deviation and the friction velocity u_* have been suggested. Thus, approximately the standard deviation of lateral (horizontal) velocity, σ_v, is equal to 2.20 u_*, and for the vertical component, σ_w is given approximately by 1.3 to 1.4u_* Then equivalent expressions to equation (3.18) for the variation with height of I_v and I_w can be derived:

$$I_v \cong 0.88/\log_e(z/z_o) \tag{3.19}$$

$$I_w \cong 0.55/\log_e(z/z_o) \tag{3.20}$$

The turbulence intensities in tropical cyclones (typhoons and hurricanes), are generally believed to be higher than those in gales in temperate latitudes. Choi (1978) found that the longitudinal turbulence intensity was about 50% higher in tropical-cyclone winds compared to synoptic winds. From measurements on a tall mast in north-western Australia during the passage of severe tropical cyclones, convective 'squall-like' turbulence was observed (Wilson, 1979). This was considerably more intense than the 'mechanical turbulence' seen closer to the ground, and was associated with the passage of bands of rain clouds.

Turbulence intensities in thunderstorm downburst winds are even less well-defined than for tropical cyclones. However, the Andrews Air Force Base event of 1983 (Figure 1.9) indicates a turbulence 'intensity' of the order of 0.1 (10%) superimposed on the underlying transient flow.

3.3.2 Probability density

As shown in Figure 3.1, the variations of wind speed in the atmospheric boundary layer are generally random in nature, and do not repeat in time. The variations are caused by eddies or vortices within the air flow, moving along at the mean wind speed. These eddies are never identical, and we must use statistical methods to describe the gustiness.

The probability density, $f_u(u_o)$, is defined so that the proportion of time that the wind velocity $U(t)$, spends in the range $u_o + du$, is $f_u(u_o).du$. Measurements have shown that the wind velocity components in the atmospheric boundary layer follow closely the Normal or Gaussian probability density function, given by equation (3.21).

$$f_u(u) = \frac{1}{\sigma_u\sqrt{2\pi}} \exp\left[-\frac{1}{2}\left(\frac{u - \bar{U}}{\sigma_u}\right)^2 \right] \tag{3.21}$$

This function has the characteristic bell shape. It is defined only by the mean value, $\bar{U}$, and standard deviation, σ_u (see also Section C3.1 in Appendix C).

Thus with the mean value and standard deviation, the probability of any wind velocity occurring can be estimated.

3.3.3 Gust wind speeds and gust factors

In many design codes and standards for wind loading (see Chapter 15), a peak gust wind speed is used for design purposes. The nature of wind as a random process means that

the peak gust within an averaging period of, say, 10 min is itself also a random variable. However, we can define an *expected*, or average, value within the 10 min period. Assuming that the longitudinal wind velocity has a Gaussian probability distribution, it can be shown that the expected peak gust, $\hat{U}$, is given approximately by equation (3.22).

$$\hat{U} = \bar{U} + g\sigma_u \tag{3.22}$$

where g is a peak factor equal to about 3.5.

Thus for various terrain, a profile of peak gust with height can be obtained. Note however, that gusts do not occur simultaneously at all heights, and such a profile would represent an envelope of the gust wind speed with height.

Meteorological instruments used for long-term wind measurements do not have a perfect response, and the peak gust wind speed they measure is dependent on their response characteristics. The response is usually indicated as an equivalent averaging time. For instruments of the pressure tube type (such as the Dines anemometer used for many years in the United Kingdom and Australia) and small cup anemometers, an averaging time of two to three seconds is usually quoted.

The *gust factor*, G, is the ratio of the maximum gust speed within a specified period to the mean wind speed. Thus is in general,

$$G = \frac{\hat{U}}{\bar{U}} \tag{3.23}$$

For gales (synoptic winds in temperate climates), the magnitude of gusts for various averaging times, τ, were studied by Durst (1960) and Deacon (1965). Deacon gave gust factors at a height of 10 metres, based on a 10-min mean wind speed, of about 1.45 for 'open country with few trees', and 1.96 for suburban terrain.

Several authors have provided estimates of gust factors over land, for tropical cyclones or hurricanes. Based on measurements in typhoons in Japan, Ishizaki (1983) proposed the following expression for gust factor, G.

$$G = \frac{\hat{U}_{s\text{sec}}}{\bar{U}_{T\text{sec}}} = 1 + 0.5\, I_u \ln(T/t) \tag{3.24}$$

where I_u is the longitudinal turbulence intensity (Section 3.3.1), T is the averaging period for the mean speed, and t is the gust duration.

A typical value of I_u at 10 m height in open country is 0.2. Then taking T equal to 600 seconds, and s equal to 2 seconds, equation (3.24) gives a value of gust factor of 1.57. A study by Krayer and Marshall (1992) of four U.S. hurricanes gave a similar value of 1.55. These values are both based on tropical cyclone winds with a wide range of wind speeds, to values as low as 10 m/s.

An analysis by Black (1992) which appeared to be based on higher wind speeds in hurricanes, gave a higher value of 1.66 for the gust factor, $\frac{\hat{U}_{2\text{ sec, 10 m}}}{\bar{U}_{10\text{ min, 10 m}}}$.

3.3.4 Wind spectra

The probability density function (Section 3.3.2) tells us something about the magnitude of the wind velocity, but nothing about how slowly or quickly it varies with time. In order

to describe the distribution of turbulence with frequency, a function called the *spectral density,* usually abbreviated to 'spectrum', is used. It is defined so that the contribution to the variance (σ_u^2, or square of the standard deviation), in the range of frequencies from n to $n + dn$, is given by $S_u(n).dn$, where $S_u(n)$ is the spectral density function for $u(t)$. Then integrating over all frequencies,

$$\sigma_u^2 = \int_0^\infty S_u(n)dn \tag{3.25}$$

There are many mathematical forms that have been used for $S_u(n)$ in meteorology and wind engineering. The most common and mathematically correct of these for the longitudinal velocity component (parallel to the mean wind direction) is the von Karman/Harris form (developed for laboratory turbulence by von Karman (1948), and adapted for wind engineering by Harris (1968)). This may be written in several forms; equation (3.26) is a commonly used non-dimensional form.

$$\frac{n.S_u(n)}{\sigma_u^2} = \frac{4\left(\frac{n\ell_u}{\bar{U}}\right)}{\left[1 + 70.8\left(\frac{n\ell_u}{\bar{U}}\right)^2\right]^{5/6}} \tag{3.26}$$

where ℓ_u is a turbulence length scale.

In this form, the curve of $n.S_u(n)/\sigma_u^2$ versus $n/\bar{U}$ has a peak; the value of ℓ_u determines the value of $(n/\bar{U})$ at which the peak occurs – the higher the value of ℓ_u, the higher the value of $(\bar{U}/n)$ at the peak, or λ, known as the 'peak wavelength'. For the von Karman-Harris spectrum, λ is equal to $6.85\ell_u$. The length scale, ℓ_u, varies with both terrain roughness and height above the ground. The form of the von Karman-Harris spectrum is shown in Figure 3.4.

The other orthogonal components of atmospheric turbulence have spectral densities with somewhat different characteristics. The spectrum of vertical turbulence is the most important of these, especially for horizontal structures such as bridges. A common math-

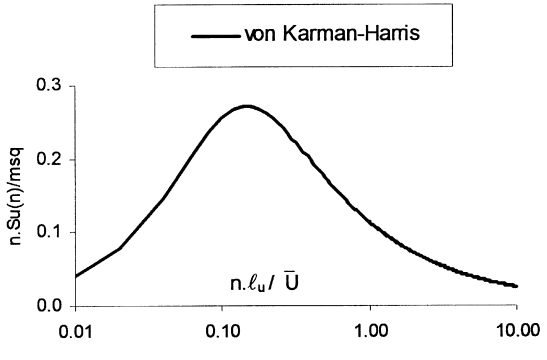

Figure 3.4 Normalised spectrum of longitudinal velocity component (von Karman-Harris).

ematical form for the spectrum of vertical turbulence (w') is the Busch and Panofsky (1968) form which can be written as equation (3.27).

$$\frac{n.S_w(n)}{\sigma_w{}^2} = \frac{2.15\left(\frac{nz}{\bar{U}}\right)}{\left[1 + 11.16\left(\frac{nz}{\bar{U}}\right)^{5/3}\right]} \tag{3.27}$$

In this case the length scale is directly proportional to the height above ground, z.

The Busch and Panofsky spectrum for vertical turbulence (w') is shown in Figure 3.5.

3.3.5 Correlation

Covariance and *correlation* are two important properties of wind turbulence in relation to wind loading. The latter is the same quantity that is calculated in linear regression analysis. In the present context, it relates the fluctuating wind velocities at two points in space, or wind pressures at two points on a building (such as a roof).

For example, consider the wind speed at two different heights on a tower (for example, Figure 3.1). The covariance between the fluctuating (longitudinal) velocities at two different heights, z_1 and z_2, is defined according to equation (3.28).

$$\overline{u'(z_1)u'(z_2)} = \frac{1}{T}\int_0^T [U(z_1,t) - \bar{U}(z_1)][U(z_2,t) - \bar{U}(z_2)]dt \tag{3.28}$$

Thus the covariance is the product of the fluctuating velocities at the two heights, averaged over time. Note that the mean values, $\bar{U}$ (z_1) and $\bar{U}$ (z_2), are subtracted from each velocity in the right-hand-side of equation (3.28). Note that in the special case when z_1 is equal

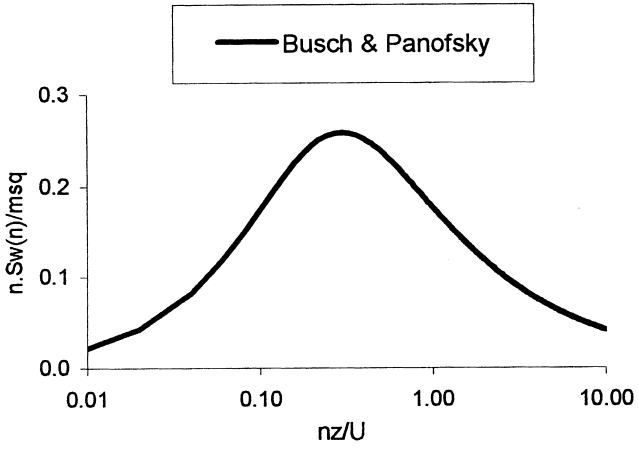

Figure 3.5 Normalised spectrum of vertical velocity component (Busch and Panofsky, 1968).

to z_2, the right-hand-side is then equal to the variance (σ_u^2) of the fluctuating velocity at the single height.

The correlation coefficient, ρ, is defined by equation (3.29).

$$\rho = \frac{\overline{u'(z_1)u'(z_2)}}{\sigma_u(z_1).\sigma_u(z_2)} \tag{3.29}$$

When z_1 is equal to z_2, the value of ρ is +1, (i.e. we have full correlation). It can be shown that ρ must lie between −1 and +1. A value of 0 indicates no correlation (i.e. no statistical relationship between the wind velocities) – this usually occurs when the heights z_1 and z_2 are widely separated.

The covariance and correlation are very useful in calculating the fluctuating wind loads on tall towers, large roofs, etc., and for estimating span reduction factors for transmission lines. In the latter case the points would be separated horizontally, rather than vertically.

A mathematical function which is useful for describing the correlation, ρ, is the exponential decay function:

$$\rho \approx \exp[-C|z_1 - z_2|] \tag{3.30}$$

This function is equal to +1 when, z_1 is equal to z_2, and tends to zero when $|z_1 - z_2|$ becomes very large (very large separations).

Figure 3.6 shows equation (3.30) with C equal to (1/40) m^{-1}. It is compared with some measurements of longitudinal velocity fluctuations in the atmospheric boundary, at a height of 13.5 m, with horizontal separations, over urban terrain (Holmes, 1973).

3.3.6 Co-spectrum and coherence

When considering the resonant response of structures to wind (Chapter 5), the correlation of wind velocity fluctuations from separated points *at different frequencies*, is important.

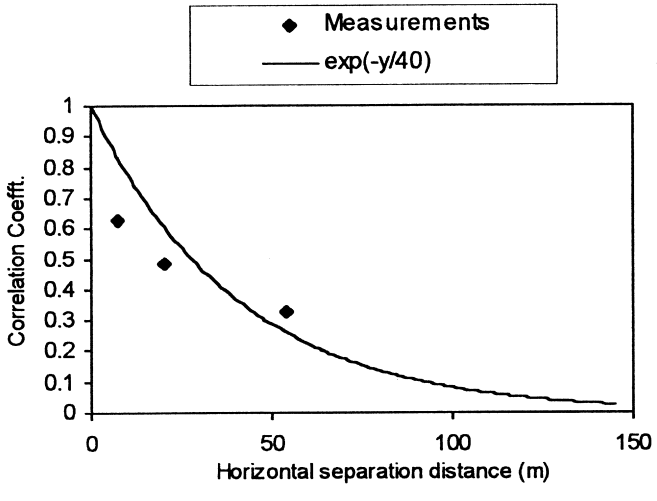

Figure 3.6 Cross-correlation of longitudinal velocity fluctuations in the atmospheric boundary layer at a height of 13.5 m (Holmes, 1973).

For example the correlations of vertical velocity fluctuations with span-wise separation, at the natural frequencies of vibration of a large-span bridge are important in determining its response to buffeting.

The frequency-dependent correlation can be described by functions known as the *cross-spectral density, co-spectral density* and *coherence*. Mathematical definitions of these functions are given by Bendat and Piersol (1999), and others. The cross-spectral density as well as being a function of frequency, is a complex variable, with real and imaginary components. The co-spectral density is the real part, and may be regarded as a frequency-dependent covariance (Section 3.3.5). The coherence is a normalized magnitude of the cross-spectrum, approximately equivalent to a frequency-dependent correlation coefficient. The normalized co-spectrum is very similar to coherence, but does not include the imaginary components; this is in fact the relevant quantity when considering the wind forces from turbulence on structures.

The normalized co-spectrum and coherence are often represented by an exponential function of separation distance and frequency:

$$\rho(\Delta z,n) = \exp\left[-\left(\frac{k.n.\Delta z}{\bar{U}}\right)\right] \tag{3.31}$$

where k is an empirical constant, used to fit measured data; a typical range of values for atmospheric turbulence is 10 to 20. Δz is the vertical separation distance. A similar function is used to represent the co-spectrum when lateral (horizontal) separations, Δy, are considered.

As for equation (3.30), equation (3.31) does not allow negative values – a theoretical problem – but of little practical significance. A more important disadvantage is that it implies full correlation at very low frequencies, no matter how large the separation distance, Δz. Since the equation only needs to be evaluated at the high frequencies corresponding to resonant frequencies, this is also not a great disadvantage.

More mathematically acceptable (but more complex) expressions for the normalized co-spectrum and coherence are available (e.g. Deaves and Harris, 1978).

3.4 Modification of wind flow by topography

Mean and gust wind speeds can be increased considerably by natural and man-made topography in the form of escarpments, embankments, ridges, cliffs and hills. These effects were the subject of considerable research in the 1970s and 1980s, with the incentive of the desire to exploit wind power, and to optimize the siting of wind turbines. This work improved greatly the prediction of mean wind speeds over shallow topography. Less well defined are the speed-up effects on turbulence and gust wind speeds, and the effects of steep topography – often of interest with respect to structural design.

3.4.1 General effects of topography

Figure 3.7 shows the general features of boundary-layer wind flow over a shallow escarpment, a shallow ridge, a steep escarpment, and a steep ridge.

As the wind approaches a shallow feature, its speed first reduces slightly as it encounters the start of the slope upwards. It then gradually increases in speed as it flows up the slope towards the crest. The maximum speed-up occurs at the crest, or slightly upwind of it.

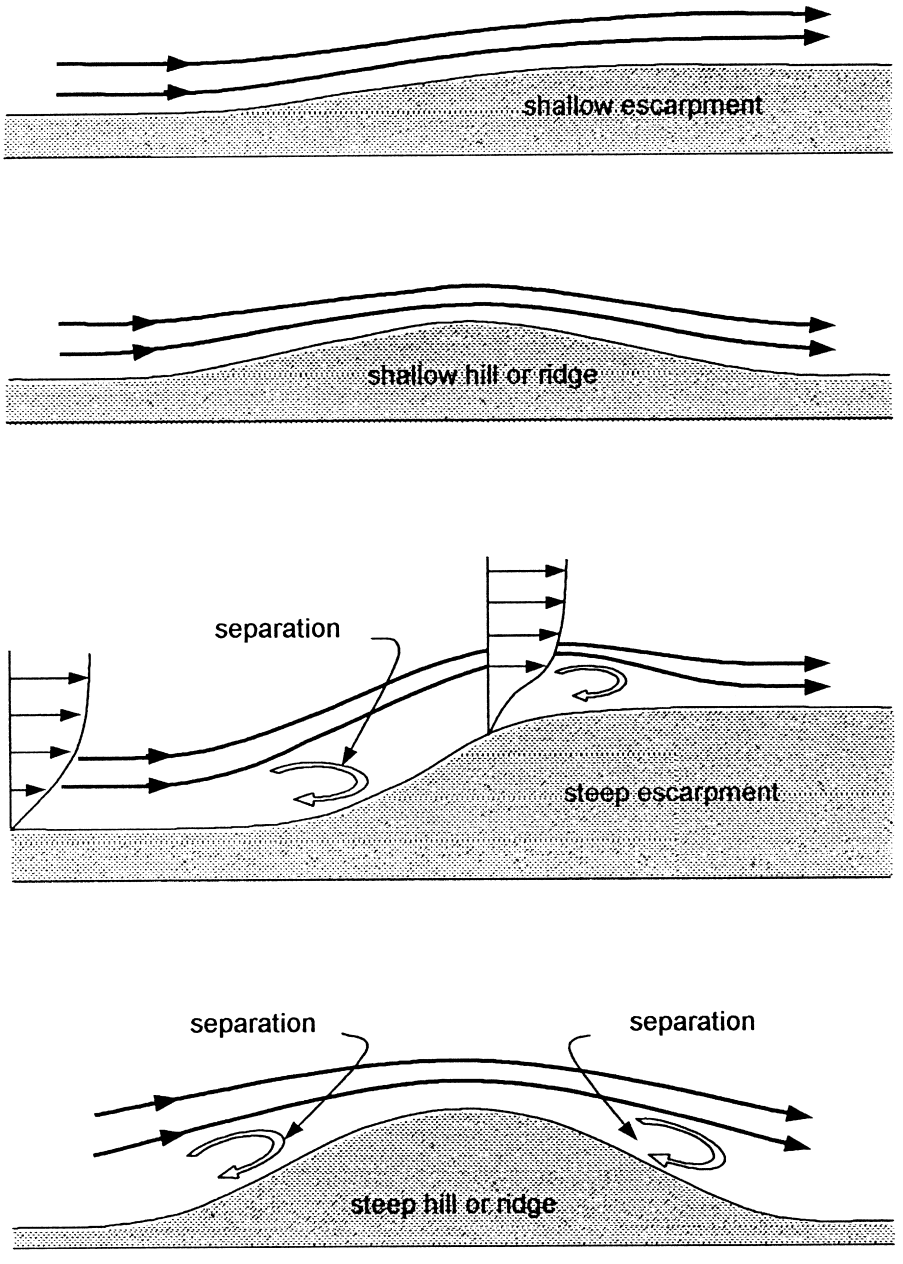

Figure 3.7 Flow over shallow and steep topography.

Beyond the crest, the flow speed gradually reduces to a value close to that well upwind of the topographic feature; the adjustment is somewhat faster for a feature with a downwind slope, such as a ridge, than for an escarpment with a plateau downwind of the crest.

On steeper features, flow 'separation' (see also Section 4.1) may occur, as the flow is not able to overcome the increasing pressure gradients in the along-wind direction. Separations may occur at the start of the upwind slope, immediately downwind of the crest, and on the downwind slope for a ridge.

For steeper slopes (greater than about 0.3), the upwind separation 'bubble' presents an 'effective slope' of approximately constant value, independent of the actual slope underneath. This is often used in codes and standards to specify an upper limit to the speed-up effects of an escarpment or ridge.

The speed-up effects are greatest near the surface, and reduce with height above the ground. This can have the effect of producing mean velocity profiles, near the crest of a topographic feature, that are nearly constant, or have a peak (see Figure 3.7).

The above discussion relates to topographic features, which are two-dimensional in nature, that is they extend for an infinite distance normal to the wind direction. This may be a sufficient approximation for many long ridges and escarpments. Three-dimensional effects occur when air flow can occur around the ends of a hill, or through gaps or passes. These alternative air paths reduce the air speeds over the top of the feature, and generally reduce the speed-up effects. For structural design purposes, it is often convenient, and usually conservative, to ignore the three-dimensional effects and to calculate wind loads only for the speed-up effects of the upwind and downwind slopes parallel to the wind direction of interest.

3.4.2 Topographic multipliers

The definition of topographic multiplier used in this book is as follows:

$$\text{Topographic Multiplier} = \frac{\text{Wind speed at height, } z\text{, above the feature}}{\text{Wind speed at height, } z\text{, above the flat ground upwind}} \tag{3.32}$$

This definition applies to mean, peak gust and standard deviation wind speeds, and these will be denoted by $\bar{M}_t$, $\hat{M}_t$ and M_t', respectively.

Topographic multipliers measured in full-scale or in wind tunnels, or calculated by computer programs, can be both greater or less than one. However in the cases of most interest for structural design, we are concerned with speed-up effects for which the topographic multiplier for mean or gust wind speeds will exceed unity.

3.4.3 Shallow hills

The analysis by Jackson and Hunt (1975) of the mean boundary-layer wind flow over a shallow hill produced the following form for the mean topographic multiplier:

$$\bar{M}_t = 1 + ks\phi \tag{3.33}$$

where ϕ is the upwind slope of the topographic feature, k is a constant for a given shape of topography and s is a position factor.

Equation (3.33) has been used in various forms for specifying topographic effects in

several codes and standards. It indicates that the 'fractional speed-up', equal to $(\bar{M}_t - 1)$, is directly proportional to the upwind slope, ϕ. The latter is defined as $H/2L_u$, where H is the height of the crest above level ground upwind, and L_u is the horizontal distance from the crest to where the ground elevation drops to $H/2$.

Taylor and Lee (1984) proposed the following values of the constant, k, for various types of topography:

- 4.0 for two-dimensional ridges
- 1.6 for two-dimensional escarpments
- 3.2 for three-dimensional (axisymmetric) hills

The position factor, s, is 1.0 close to the crest of the feature, and falls upwind and downwind and with height, z, above local ground level. The reduction of s with height is more rapid near the ground, becoming more gradual as z increases.

To a first approximation, the longitudinal turbulence component, σ_u, does not change over the hill or escarpment. This results in the following equation for the gust topographic multiplier, $\hat{M}_t$:

$$\hat{M}_t = 1 + k' s \phi \tag{3.34}$$

where k' is a constant for the gust multiplier, related to k by equation (3.35).

$$k' = \frac{k}{1 + g\left(\frac{\sigma_u}{\bar{U}}\right)} \tag{3.35}$$

$\left(\frac{\sigma_u}{\bar{U}}\right)$ is the longitudinal turbulence intensity (over flat level ground) defined in Section 3.3.1, and g is the peak factor (Section 3.3.3).

Equations (3.33) to (3.35) show that the gust topographic multiplier is lower than the mean topographic multiplier for the same type of topography and height above the ground.

There is a slight dependence of the topographic multipliers on the Jensen Number (Section 4.4.5) based on the hill height, (H/z_0).

3.4.4 Steep hills, cliffs and escarpments

Once the upwind slope of a hill or escarpment reaches a value of about 0.3 (about 17 degrees), separations occur on the upwind face (Figure 3.7) and the simple formulae given in Section 3.4.3 cannot be applied directly.

For slopes between about 0.3 and 1 (17 to 45 degrees), the separation bubble on the upwind slope presents an effective slope to the wind which is relatively constant, as discussed in Section 3.4.1. The topographic multipliers, at or near the crest, are therefore also fairly constant with upwind slope in this range. Thus for this range of slopes, equations (3.33) and (3.34) can be applied with ϕ replaced by an effective slope ϕ', equal to about 0.3 (Figure 3.8).

For slopes greater than about 1, for example steep cliffs, the flow stream lines near ground level at the crest, originate from the upwind flow at levels near cliff height above the upwind ground level, rather than near ground level upwind (Figure 3.9). The concept

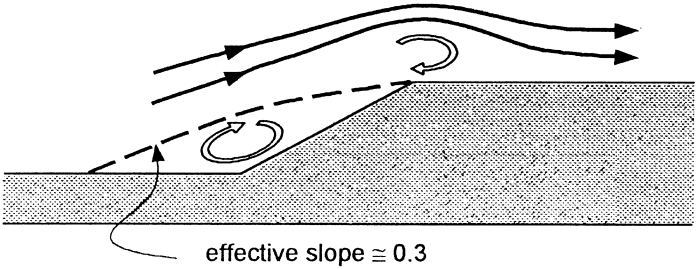

Figure 3.8 Effective upwind slope for steep escarpments.

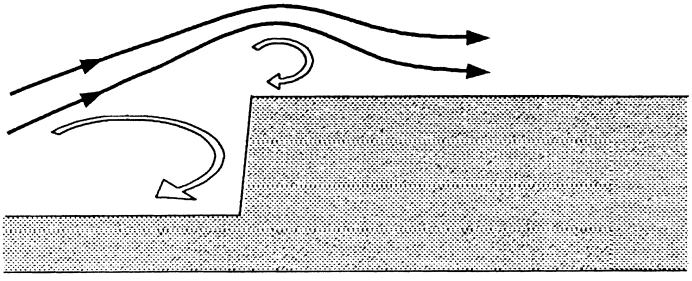

Figure 3.9 Wind flow over a steep cliff.

of the topographic multiplier as defined by equation (3.32) is less appropriate in such cases. Some of the apparent speed-up is caused by the upstream boundary layer profile rather than a perturbation produced by the hill or cliff.

An additional complication for steep features is that separations can occur at or down wind of the crest (see Figure 3.7). Separated flow was found within the first 50 m height above the crest of a 480 m high feature, with an upwind slope of only 0.48 (average angle of 26 degrees), in both full scale, and 1/1000 scale wind-tunnel measurements (Glanville and Kwok, 1997). This has the effect of decreasing the mean velocity, and increasing the turbulence intensity, as shown in Figure 3.10.

3.4.5 Effect of topography on tropical cyclones and thunderstorm winds

The effect of topographic features on wind near the ground in tropical cyclones and thunderstorm downbursts is much less clearly understood than those in the well-developed boundary-layers of large scale synoptic systems.

Tropical cyclones are large storms with similar boundary layers to extra-tropical depressions on their outer edges. Near the region of strongest winds, they appear to have much lower boundary-layer heights – of the order of 100 m. Topographic features greater than this height would therefore be expected to interact with the structure of the storm itself.

Thunderstorm downdrafts also have 'boundary-layers' with peaks in the velocity profiles at 50–100 m. They also do not have fully-developed boundary-layer velocity profiles. There have been some basic studies using wind-tunnel jets impinging on a flat board

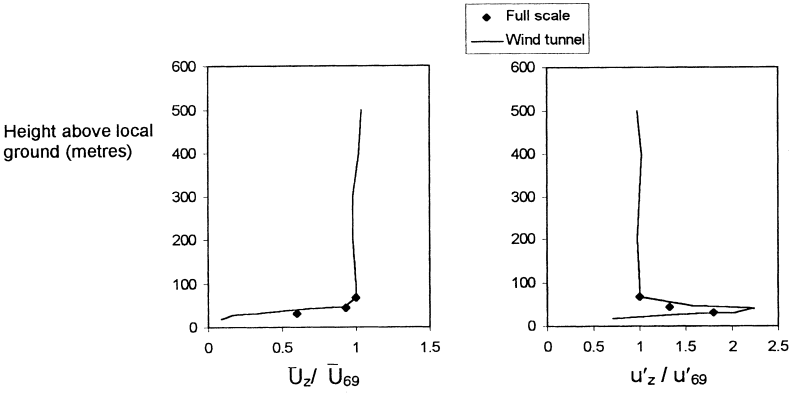

Figure 3.10 Mean velocity profile and r.m.s. longitudinal turbulent velocity near the crest of a steep escarpment (H = 480 m, upwind slope = 0.48).

(Letchford and Illidge, 1999; Wood *et al.*, 1999) to indicate considerably lower topographic multipliers compared with developed thick boundary-layer flows. However the effect of forward motion of the storm may modify these conclusions.

3.5 Change of terrain

When strong winds in a fully-developed boundary layer encounter a change of surface roughness, for example winds from open country flowing over the suburbs of a town or city, a process of adjustment in the turbulent boundary-layer flow properties develops. The adjustment starts at ground level and gradually moves upwards. The result is the development of an internal boundary layer over the new terrain as shown in Figure 3.11.

Deaves (1981), from numerical studies, developed the following relationships for the horizontal position of the inner boundary layer as a function of its height, z:

For flow from smooth terrain (roughness length z_{o1}) to rougher terrain (z_{o2}) with $z_{o2} > z_{o1}$:

$$x_i(z) = z_{o2}\left(\frac{z}{0.36z_{o2}}\right)^{4/3} \tag{3.36}$$

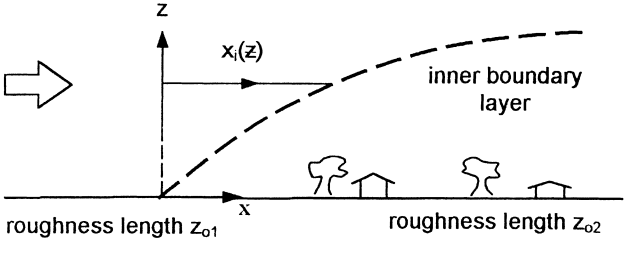

Figure 3.11 Internal boundary-layer development at a change of terrain roughness.

For flow from rough terrain (roughness length z_{o1}) to smoother terrain (z_{o2}) with $z_{o1} > z_{o2}$:

$$x_i(z) = 14z\left(\frac{z_{o1}}{z_{o2}}\right)^{\frac{1}{2}} \tag{3.37}$$

Setting z_{o2} equal to 0.2 m, approximately the value for suburban terrain with low rise buildings 3 to 5 m high (see Table 3.1), and z equal to 10 m, equation (3.36) gives a value for $x_i(10)$ of 144 m. Beyond this distance, the shape of the mean velocity profile below 10 m has the characteristics of the new terrain. However the *magnitude* of the mean velocity continues to reduce for many kilometres, until the complete atmospheric boundary layer has fully adjusted to the rougher terrain.

Melbourne (1992) found the *gust* wind speed at a height of 10 m, adjusts to a new terrain approximately exponentially with a distance constant of about 2000 m. Thus the peak gust at a distance x (in metres) into the new terrain (2) can be represented by equation (3.38).

$$\hat{U}_{2,x} = \hat{U}_1 + (\hat{U}_2 - \hat{U}_1)\left[1 - \exp\left(\frac{-x}{2000}\right)\right] \tag{3.38}$$

where $\hat{U}_1$ and $\hat{U}_2$ are the asymptotic gust velocities over fully-developed terrain of type 1 (upstream) and 2 (downstream).

Equation (3.38) was found to fit data from a wind tunnel for flow from rough to smooth, as well as smooth to rough, and when there were several changes of roughness.

3.6 Other sources

A well-documented and detailed description of the atmospheric boundary in temperate synoptic systems, for wind loading purposes, is given in a series of data items published by the Engineering Sciences Data Unit (ESDU (1974–99). These include the effects of topographic and terrain changes. The mathematical model of atmospheric turbulence in temperate gale conditions of Deaves and Harris (1978), which used data only from measurements which satisfied rigorous conditions, such as very uniform upstream terrain, is also well known, and contains mathematically acceptable expressions for turbulence quantities in the atmospheric boundary layer. Cook (1985) has described, for the designer, a structure of the atmospheric boundary layer, which is consistent with the above models.

These references are strongly recommended for descriptions of strong wind structure in temperate zones. However, as discussed in this chapter, the strong wind structure in tropical and semi-tropical locations, such as those produced by thunderstorms and tropical cyclones, is different, and such models should be used with caution in these regions.

3.7 Summary

In this chapter, the structure of strong winds near the earth's surface, relevant to wind loads on structures, has been described. The main focus has been the atmospheric boundary layer in large synoptic winds over land. The mean wind speed profile and some aspects of the turbulence structure has been described. However some aspects of wind over the oceans, and in tropical cyclones and thunderstorm downbursts, have also been discussed.

The modifying effects of topographic features and of changes in terrain have also been briefly covered.

References

Amano, T., Fukushima, H., Ohkuma, T., Kawaguchi, A. and Goto, S. (1999) 'The observation of typhoon winds in Okinawa by Doppler sodar', *Journal of Wind Engineering and Industrial Aerodynamics* 83: 11–20.

Bendat, J. S. and Piersol, A. G. (1999) *Random Data: Analysis and Measurement Procedures*, 3rd edn. New York: J. Wiley.

Black, P. G. (1992) 'Evolution of maximum wind estimates in typhoons', *ICSU/WMO Symposium on Tropical Cyclone Disasters*, October 12–18, Beijing, China.

Busch, N. and Panofsky, H. (1968) 'Recent spectra of atmospheric turbulence', *Quarterly Journal of the Royal Meteorological Society* 94: 132–48.

Charnock, H. (1955) 'Wind stress on a water surface', *Quarterly Journal of the Royal Meteorological Society* 81: 639–40.

Choi, E. C. C. (1978) 'Characteristics of typhoons over the South China Sea', *Journal of Industrial Aerodynamics* 3: 353–65.

Cook, N. J. (1985) *The Designer's Guide to Wind Loading of Building Structures. Part 1 Background, Damage Survey, Wind Data and Structural Classification*. London: Building Research Establishment and Butterworths.

Deacon, E. L. (1955) 'Gust variation with height up to 150 metres', *Quarterly Journal of the Royal Meteorological Society* 81: 562–73.

—— (1965) 'Wind gust speed: averaging time relationship', *Australian Meteorological Magazine* 51: 11–14.

Deaves, D. M. (1981) 'Computations of wind flow over changes in surface roughness', *Journal of Wind Engineering and Industrial Aerodynamics* 7: 65–94.

Deaves, D. M. and Harris, R. I. (1978) A mathematical model of the structure of strong winds. Construction Industry Research and Information Association (U.K.), Report 76.

Durst, C. S. (1960) 'Wind speeds over short periods of time', *Meteorological Magazine* 89: 181–6.

E.S.D.U. (1974–99) Wind speeds and turbulence. Engineering Sciences Data Unit (ESDU International), Wind Engineering series Volumes 1a and 1b. ESDU Data Items 74030, 82026, 83045, 84011, 84031, 85020, 86010, 86035, 91043, 92032.

Fujita, T. T. (1985) *The Downburst. Report on Projects NIMROD and JAWS*. Published by the author at the University of Chicago.

Garratt, J. R. (1977) 'Review of drag coefficients over oceans and continents', *Monthly Weather Review* 105: 915–29.

Glanville, M. J. and Kwok, K. C. S. (1997) 'Measurements of topographic multipliers and flow separation from a steep escarpment. Part II. Model-scale measurements', *Journal of Wind Engineering and Industrial Aerodynamics* 69–71: 893–902.

Harris, R. I. (1968) 'On the spectrum and auto-correlation function of gustiness in high winds', Electrical Research Association. Report 5273.

Holmes, J. D. (1973) 'Wind pressure fluctuations on a large building', Ph.D. thesis, Monash University, Australia.

Ishizaki, H. (1983) 'Wind profiles, turbulence intensities and gust factors for design in typhoon-prone regions', *Journal of Wind Engineering and Industrial Aerodynamics* 13: 55–66.

Jackson, P. S. and Hunt, J. C. R. (1975) 'Turbulent flow over a low hill', *Quarterly Journal of the Royal Meteorological Society* 101: 929–55.

Krayer, W. R. and Marshall, R. D. (1992) 'Gust factors applied to hurricane winds', *Bulletin, American Meteorological Society* 73: 613–17.

Letchford, C. W. and Illidge, G. (1999) 'Turbulence and topographic effects in simulated thunderstorm downdrafts by wind tunnel jet', *Proceedings, 10th International Conference on Wind Engineering*, Copenhagen, Denmark, 21–24 June 1999, Balkema, Rotterdam.

Lettau, H. H. (1959) 'Wind profile, surface stress and geostrophic drag coefficients in the atmospheric boundary layer', *Proceedings, Symposium on Atmospheric Diffusion and Air Pollution*, Oxford, U.K., Academic Press, New York.

Melbourne W. H. (1992) Unpublished course notes, Monash University.

Oseguera, R. M. and Bowles, R. L. (1988) 'A simple analytic 3–dimensional downburst model based on boundary layer stagnation flow', *N.A.S.A. Technical Memorandum 100632,* National Aeronautics and Space Administration, Washington. D.C.

Taylor, P. A. and Lee, R. J. (1984) 'Simple guidelines for estimating windspeed variation due to small scale topographic features', *Climatological Bulletin* (Canada) 18: 3–32.

von Karman, T. (1948) 'Progress in the statistical theory of turbulence', *Proceedings of the National Academy of Sciences (U.S.)* 34: 530–9.

Wilson, K. J. (1979) 'Characteristics of the subcloud layer wind structure in tropical cyclones', *International Conference on Tropical Cyclones*, Perth, Western Australia, November 1979.

Wood, G. S., Kwok, K. C. S., Motteram, N. and Fletcher, D. F. (1999) 'Physical and numerical modelling of thunderstorm downbursts', *Proceedings, 10th International Conference on Wind Engineering*, Copenhagen, Denmark, 21–24 June 1999, Balkema, Rotterdam.